

NUCLEAR QUADRUPOLE RESONANCE IN SOLIDS *

BY H. G. DEHMELT

Dept. of Physics, Duke University, Durham, N.C., U.S.A.

Received 8th February, 1955

Nuclear quadrupole resonance—also called pure electric quadrupole spectra—is a recently developed branch of radio-frequency spectroscopy. It is concerned with magnetic resonance absorption in crystals. This absorption is due to reorientation of the non-spherical atomic nuclei against crystalline electric fields. Related phenomena in free molecules are briefly discussed. This is followed by a treatment of the electrostatic interaction of a non-spherical nucleus with an axially symmetric electric field. Such a field is found, e.g. in crystalline Cl_2 , a crystal whose structural units are very nearly undisturbed Cl_2 molecules. Electrostatic torques are shown to exist, which cause a precession of the nuclear angular momenta around the molecular axes. This motion is accompanied by a precession of the magnetic and electric moments of the nuclei, which may interact with alternating electromagnetic fields of the proper frequency. Thus one arrives at the transition mechanism between energy levels which are derived from the corresponding Hamiltonian. Then some experimental aspects are described and examples of absorption lines are given. The significance of the experimental information obtained, namely, the quadrupole coupling constant eQq_{zz} and the asymmetry parameter

$$\epsilon = |(q_{xx} - q_{yy})/q_{zz}|,$$

is pointed out. The fundamental point is emphasized that these quantities are characteristic of the electron density distribution around a *single* nucleus which is closely related to the bonding of the corresponding atom. The advantages and disadvantages of quadrupole resonance studies are discussed. It is seen that the class of dipole-less

* supported by the Office of Ordnance Research.

molecules which exhibits no rotational spectra is well suited for this method, as interactions between neighbouring molecules are small here. This class comprises all element molecules and highly symmetrical molecules which are especially accessible to structural analysis. The recent determinations of the quadrupole couplings for the halogen molecules Cl_2 , Br_2 and I_2 —important because of their simplicity—contributed materially to the understanding of their structure. Furthermore, a multitude of molecules, molecular addition compounds, molecular ions as well as crystals with covalently bonded lattices, which can be obtained in the gaseous state only with difficulty or not at all, are most conveniently studied by quadrupole resonance and typical cases are given. Finally, all atoms investigated by this method are reviewed.

1. INTRODUCTION

Nuclear quadrupole resonance (NQR), a recently developed¹⁻⁴ branch of radio-frequency spectroscopy, has already contributed significant information on molecular and crystalline structure. Experimentally, it is concerned with the detection of radio-frequency magnetic resonance absorption in suitable crystals. In this and many other respects it is similar to nuclear magnetic resonance (NMR).^{5,6} However, while in nuclear magnetic resonance one has to do with transitions between levels corresponding to different orientations of the nuclear magnetic moments against a static field applied from the outside, no such field is needed in NQR. The place of the magnetic field is taken by an inhomogeneous (axially symmetric) electric field generated by the charge cloud of the (diatomic) molecule containing the nucleus. This electric field now interacts with the electric quadrupole moment of the nucleus instead of its magnetic dipole moment. The quadrupole moment measures the deviation from spherical symmetry of the nuclear charge distribution. Again, different relative orientations of nuclear axis against field axis correspond to different energy levels. For free molecules such nuclear quadrupole effects have been observed earlier in molecular beam resonance experiments⁷ and in rotational absorption spectra in the microwave region,⁸ where they lead to a hyperfine structure of the lines.

2. MOTION AND ENERGY EIGENVALUES IN A QUADRUPOLE SYSTEM^{9,10}

We now consider in more detail a system which consists of a non-spherical nucleus in a diatomic molecule forming part of a molecular crystal, to be specific, one Cl nucleus in solid Cl_2 . In such a crystal the molecules essentially retain their identity and the electrostatic field generated at the site of the Cl nucleus is practically determined by the molecular electron cloud alone. Therefore it is very nearly axially symmetric, even though the surroundings in the lattice have lower symmetry. We introduce a frame of reference xyz fixed in space (see fig. 1), the z -axis coinciding with the molecular axis and in the point of origin the Cl nucleus under consideration, which in fig. 1 and 2 is represented as a highly enlarged ellipsoid. Further, a second frame x', y', z' with z' fixed along the nuclear axis is chosen. Since both nucleus and surrounding molecular field q are axially symmetric, the electrostatic interaction energy

$$W = \int \rho_N q dV \quad (2.1)$$

can only depend on the angle θ between nuclear and molecular axis. To simplify the calculation we therefore let the y and y' axes fall together. Quantity ρ_N denotes the charge distribution in the nucleus. If the potential q as function of $x'y'z'$ is expanded around the origin. W takes the form

$$\begin{aligned} W = & q(0) \int \rho_N dV' + q_{x'x'}(0) \int \rho_N x'^2 dV' + \dots \\ & + \frac{1}{2} [q_{x'y'}(0) \int \rho_N x'y' dV' + q_{y'y'}(0) \int \rho_N y'^2 dV' \\ & + q_{z'z'}(0) \int \rho_N z'^2 dV'] + \dots \end{aligned} \quad (2.2)$$

The first constant term in this expression is of no interest to us. The following (dipole) terms containing the first derivatives of q vanish, as the integrals are zero because of the symmetry of the nucleus. The (quadrupole) terms with the second derivatives of q are the ones of interest, while higher terms can be neglected in excellent approximation as proven by the experiments. Since the integrals $\int \rho_N x'^2 dV' \dots$ constitute the components of a tensor—henceforth abbreviated $eQ_{x'x'}$, $eQ_{y'y'}$. . .—whose principal axes coincide with x' , y' , z' , no mixed terms

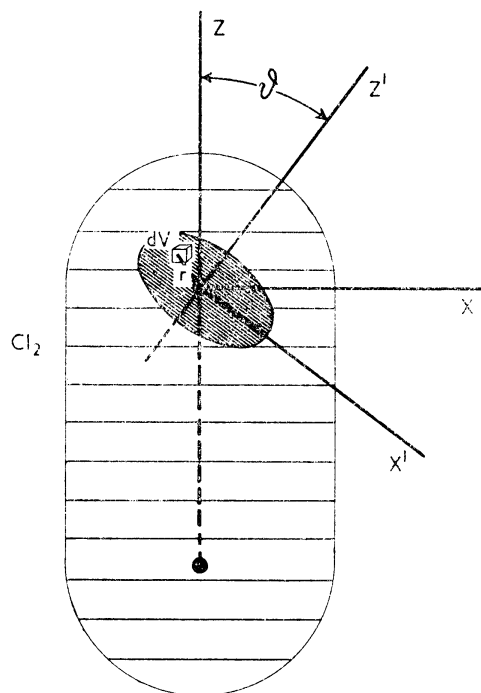


FIG. 1.—Non-spherical Cl nucleus in Cl₂ molecule.

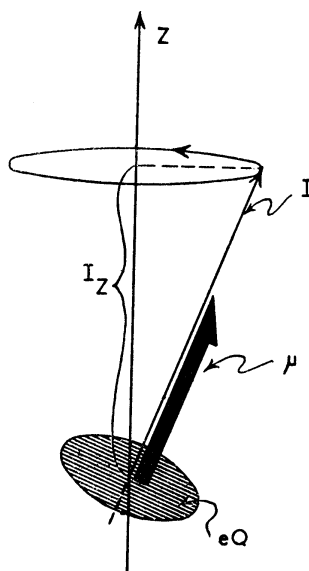


FIG. 2.—Precession of nuclear moments I , μ , eQ around symmetry axis of molecular electric field.

$Q_{x'y'}$, $Q_{x'z'}$, $Q_{y'z'}$ appear in formula (2.2). Without referring to their tensor character, it can also be seen directly that these integrals $\int \rho_N x' y' dV \dots$ vanish for the assumed symmetry of the nucleus. We now make use of the Laplace equation $q_{x'x'} + q_{y'y'} + q_{z'z'} = 0$ holding at the site of the nucleus. With $Q_{x'x'} = Q_{y'y'}$ because of the axial symmetry we obtain for the quadrupole interaction energy,

$$W_Q = \frac{1}{2} e q_{z'z'} (Q_{z'z'} - Q_{x'x'}). \tag{2.3}$$

This reduces to

$$W_Q = \frac{1}{4} q_{z'z'} \int \rho_N (3z'^2 - r^2) dV', \tag{2.4}$$

since

$$\int \rho_N x'^2 dV' = \frac{1}{2} \int \rho_N (r^2 - z'^2) dV'.$$

The integral $\int \rho_N (3z'^2 - r^2) dV'$ defines an inherent property of the nucleus and is customarily called “the” nuclear quadrupole moment and denoted by eQ . It measures the deviation from spherical symmetry of the nuclear charge cloud. A nucleus elongated with respect to its axis has a positive, a flattened nucleus a negative quadrupole moment. For a spherical nucleus eQ vanishes of course.

Quantity $q_{z'z'}$ in eqn. (2.4) can be expressed as

$$q_{z'z'} = q_{xx} \sin^2 \theta + q_{zz} \cos^2 \theta, \quad (2.5)$$

with $q_{xx} = q_{yy} = -\frac{1}{2}q_{zz}$ this reduces to

$$q_{z'z'} = q_{zz} \left(\frac{3}{2} \cos^2 \theta - \frac{1}{2} \right). \quad (2.6)$$

Here q_{zz} represents an inherent molecular quantity which, because of the axial symmetry, completely suffices to describe the electric field at the site of the nucleus. Finally we have obtained for the classical quadrupole interaction energy the formula

$$W_Q = \frac{1}{4} eQq_{zz} \left(\frac{3}{2} \cos^2 \theta - \frac{1}{2} \right). \quad (2.7)$$

Because of the dependence of the energy W_Q on θ there must result a torque, which for the appropriate sign of eQq_{zz} tends to align the nuclear and the molecular axes. As in the Zeeman effect, the nuclear angular momentum I , whose direction coincides with the figure axis of the nucleus, will respond to this torque by a precession around the z -axis (see fig. 2). However, while in the Zeeman effect the precession frequency is constant, independent of θ , we find for the quadrupole system a precession which slows down with growing θ , comes to a standstill for $\theta = \pi/2$, reverses its sense and between $\theta = \pi/2$ and π again increases in frequency. Quantum mechanically this is reflected in the spacing of the energy levels, which is not equidistant as in the Zeeman effect, but increases with growing values of the magnetic quantum number m . This precession of the angular momentum—compare fig. 2—will also be accompanied by rotating components of the magnetic dipole μ , as well as the electric quadrupole moment eQ of the nucleus, which in the classical picture must lead to the respective radiations. It can be seen, however, that only the rotating magnetic dipole experiences any appreciable coupling with an electromagnetic radiation field of the appropriate low frequency of a few megacycles while the coupling of the electric quadrupole is many orders of magnitude smaller.

Now we shall try to derive the quantum-mechanical energy eigenvalues of our quadrupole system—abbreviated QS. We note that the z component of the angular momentum I_z is a constant of the motion—compare fig. 2—whose eigenvalues m therefore can be used to label the energy eigenvalues of the QS. By substituting the operators I_z/I for $\cos \theta$ in the classical expression (2.7) we obtain the Hamiltonian

$$\mathbf{H} = \frac{1}{8} eQ^* q_{zz} (3I_z^2 - I^2)/I^2, \quad (2.8)$$

from which follow the energy eigenvalues

$$E_m = \frac{1}{8} eQ^* q_{zz} [3m^2 - I(I+1)]/I(I+1). \quad (2.9)$$

In eqn. (2.9), Q has been marked with an asterisk in order to show that in this formula it has been evaluated with respect to the figure axis of the nucleus. This deviates somewhat from the customary definition of the nuclear quadrupole moment Q , which is to be taken for the aligned state $m = I$ of the nucleus with respect to the axis of alignment z . Even though quantum-mechanically complete alignment is not possible, the charge distribution $\rho_{m=I}$ is axially symmetric with respect to the z axis, the axis of the electric field. This is due to the fact that $\rho_{m=I}$ represents an average of the nuclear charge distribution over the motion which has not completely ceased even for $m = I$. In this case the interaction energy can easily be written down independent of eqn. (2.9) using eqn. (2.4) for $\theta = 0$ and substituting $\rho_{m=I}$ for ρ_N . Thus we obtain for the energy eigenvalue $E_{m=I}$:

$$E_{m=I} = \frac{1}{4} q_{zz} \int \rho_{m=I} (3z^2 - r^2) dV. \quad (2.10)$$

Here the integral is identical with the customary eQ . Comparing this with E_I from eqn. (2.9) we find

$$Q^* = 2Q(I+1)/(2I-1). \quad (2.11)$$

Since the square of the total nuclear angular momentum is a constant of the system, we can substitute for the operator I^2 in the denominator of eqn. (2.8) its eigenvalue $I(I+1)$, and using eqn. (2.11) we obtain from eqn. (2.8) and (2.9) the final expressions

$$\mathbf{H} = eQq_{zz}(3I_z^2 - I^2)/4(2I - 1)I, \tag{2.12}$$

and

$$E_m = eQq_{zz}[3m^2 - I(I + 1)]/4(2I - 1)I. \tag{2.13}$$

The energy levels following from eqn. (2.13) are sketched in fig. 3 for integer and half-integer I values. For $I \leq \frac{1}{2}$ the quadrupole interaction energy vanishes. This follows from formula (2.11) for $I = \frac{1}{2}$ while for $I = 0$ the nuclear charge distributing in eqn. (2.10) becomes spherically symmetric which reduces the integral to zero.

In case the axial symmetry of the electric field is only approximate, an asymmetry parameter may be defined:

$$\epsilon = |(q_{xx} - q_{yy})/q_{zz}|. \tag{2.14}$$

This asymmetry causes, as a perturbation calculation shows, a first-order splitting only of the degenerate $m = \pm 1$ levels, while all other levels experience only small second-order shifts.¹¹⁻¹³ In all cases ϵ can be determined from the observed spectra, provided a Zeeman effect is produced for $I = \frac{3}{2}$.²²

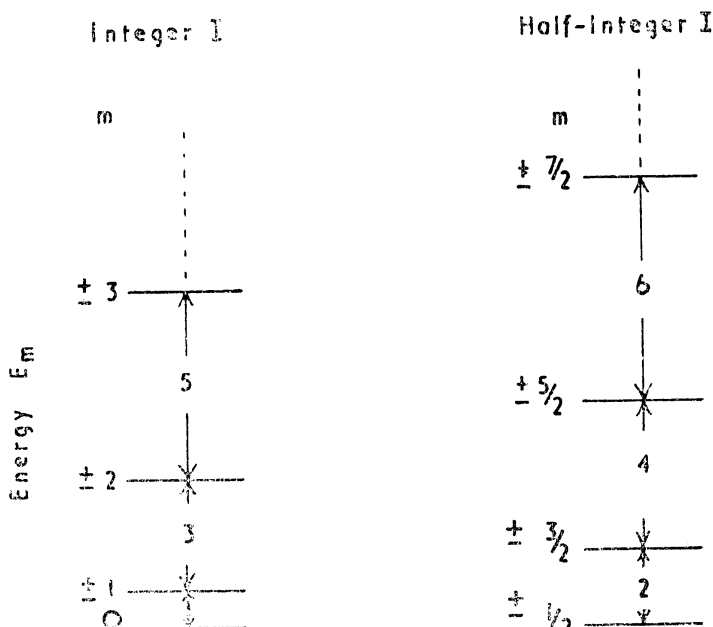


FIG. 3.—Energy levels arising from the interaction of a quadrupole nucleus with an axially symmetric electric field. The diagram is drawn for $eQq_{zz} > 0$, the unit of energy being $3eQq_{zz}/(4I - 1)$.

3. TRANSITIONS AND R.F. SUSCEPTIBILITY⁵

In order to bring about transitions between these energy levels which we have just described, we apply a magnetic r.f. field perpendicular to the z -axis whose frequency corresponds to the energy difference between two consecutive levels (selection rule $\Delta m = \pm 1$). The action of the magnetic r.f. field can be understood best by decomposing it in two oppositely rotating components. While the component whose sense of rotation is identical with that of the nuclear precession in the classical picture exerts a steady torque on the nuclear magnetic moment which changes the angle of the precession cone, the effects of the other component average out. The energy which the spin system is able to extract from

the r.f. field in this way is then dissipated into the crystal lattice through relaxation processes. This absorption is conveniently described by an imaginary r.f. susceptibility of the sample whose magnitude is given by

$$\chi'' = \frac{2}{3} \frac{N_0 \mu^2}{(2I+1)kT} \frac{I(I+1) - mm'}{I^2} \frac{\nu}{\Delta\nu} \quad (3.1)$$

In this formula N_0 denotes the number of nuclei per cm^3 and μ their magnetic moment. The frequency of the absorption line and its width between half-power points are given by ν and $\Delta\nu$. The temperature T enters, since only half of the small surplus in the lower of the Boltzmann populated levels can be lifted up in the higher one before stimulated emission completely cancels absorption. The ratio of 2π times the r.f. energy stored in the volume of the sample to the energy absorbed per cycle, which is commonly called the Q of the sample is connected with χ'' by the relation

$$\chi'' = 1/4\pi Q. \quad (3.2)$$

Here χ'' has been given for a polycrystalline material, in which the axes of the molecular electrical fields are randomly oriented with respect to the linear r.f. field.

It might be emphasized that no single crystals are required in NQR which greatly adds to the convenience of such experiments.

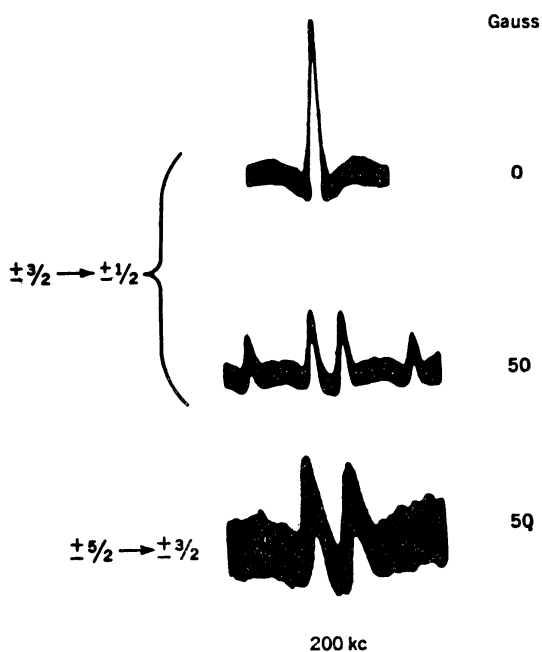


FIG. 4.—NQR absorption line due to the ^{127}I nuclei in SnI_4 (from ref. (16)). 50 c/s capacitive frequency modulation and oscilloscopic display was used. The two lower traces show the Zeeman pattern for both of the occurring transitions. The frequency scale for all three traces is the same.

4. EXPERIMENTAL ASPECTS

Exactly as in NMR, NQR absorption lines are detected by making the sample the core of a r.f. coil which is part of a tank circuit and displaying in some way the reduction of the Q of this circuit when it is tuned over an absorption line. However, as opposed to NMR where it is possible to keep the frequency constant and shift the energy levels by varying the static magnetic field, in NQR experiments the spectrometer must have a sufficiently wide frequency range. This calls for simple and easily tunable circuits. The effects to be detected are not strong and can easily be lost in the noise generated in the tubes and other parts of the detection circuit. In a good spectrometer the noise is essentially only the thermal noise of the tank circuit

containing the sample. However, at the same time the circuit should be able to develop a r.f. power as high as possible, since the absorbed power is proportional to the r.f. power incident upon the sample. While regenerative oscillators^{14, 15} are quite satisfactory at low power levels, they do not allow the generation of higher r.f. powers without generating an excessive amount of tube noise at the same time so that nothing in signal-to-noise ratio can be gained in this way. In NMR this is not too serious, as the early onset of saturation in the small samples usually employable forbids the use of higher power anyway. A different situation is encountered in NQR where in many cases saturation can

easily be avoided by the use of large samples or need not be feared because short relaxation times are to be expected. Here the use of super-regenerative oscillators ^{16,17} has proven especially advantageous. The obvious shortcomings of these circuits are not serious as long as the experimental aim is not the exact measurement of line shapes or relaxation times, but highest sensitivity in detecting unknown lines.

Higher sensitivity of course can be achieved by reducing the band width of the amplifying circuits in order to suppress the noise. While capacitive modulation can also be used in conjunction with narrow band recording circuits,

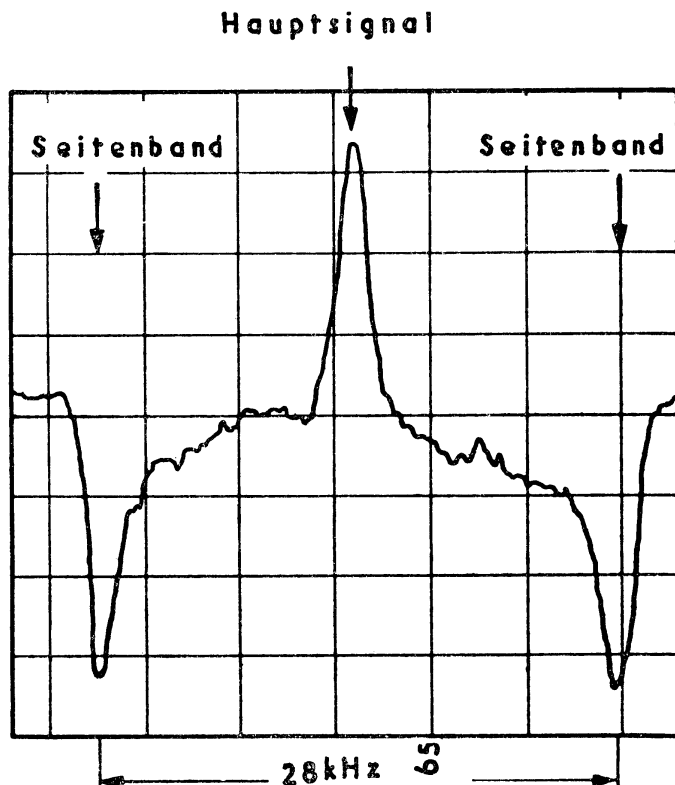


FIG. 5.—Recording of the NQR absorption line in polycrystalline $B(CH_3)_3$ at 2589.0 kc/s (from ref. (18)). The line corresponds to the transitions $m = \pm 2 \rightarrow \pm 3$ of the ^{10}B isotope. 30 c/s Zeeman modulation and a lock-in amplifier employing a time constant of 40 sec were used.

if a few precautions are taken, it appears more satisfactory to use Zeeman modulation ^{18,19} of the nuclei. With this type of modulation the lines in a polycrystalline sample are periodically smeared out by zero based field pulses of about 100 gauss. No previous knowledge of the line width is necessary to obtain optimum modulation efficiency, and response to spurious signals is greatly reduced also.

5. DISCUSSION OF INFORMATION OBTAINABLE FROM NQR EXPERIMENTS

As frequencies in the r.f. region can easily be measured with accuracies of 10^{-5} or better, the coupling constants eQq_{zz} can be obtained from NQR spectra with comparable accuracy, provided the asymmetry ϵ is known. For nuclei with spins other than $I = 3/2$ this parameter can also be deduced from the spectrum with considerable accuracy. Quite generally these two quantities provide information on the shape and density of the electron cloud in the neighbourhood

of a *single* (quadrupole) nucleus, as (in the axially symmetric case) q_{zz} can be expressed as

$$q_{zz} = \int \rho_{\text{electron}} R^{-3} (3 \cos^2 \theta - 1) dV \quad (5.1)$$

containing the electron-nucleus distance R in the inverse cube. As ϵ and eQq_{zz} are closely related to the electron-configurations around a *single* quadrupole atom which, in turn, is characteristic of the state of bonding of this atom^{20, 21} these data frequently turn out to be of a more fundamental character than other molecular quantities like dipole moments, bond distances and force constants which are of a more complex nature involving two or more atoms.

How well the NQR data can be interpreted now depends naturally upon how well the make-up of the whole crystal, which contains the quadrupole atoms, can be understood. Also in order to realize the full value of NQR data the corresponding couplings for the free atoms should be known which, however, is not the case always.

Purely practical reasons appear to limit NQR experiments to crystals in which the atoms of interest are covalently bonded to one or more neighbour-atoms, because only in these cases the NQR frequencies are likely to be high enough to allow their observation. The small quadrupole effects occurring for atomic ions with inert gas configurations are usually more conveniently observed with NMR techniques.²

We shall now try to illustrate, with the help of some selected cases, to what kind of problems NQR has been applied, and to what use the experimental results may be put. One might begin with the rather general type of information which the experiments provide, like the number and symmetry of non-equivalent lattice sites in a crystal¹⁶ which are occupied by the same atomic species but generally do not have identical q_{zz} values. Furthermore, when single crystals are available the Zeeman effect¹¹⁻¹³ of NQR lines can be used in determining the direction of

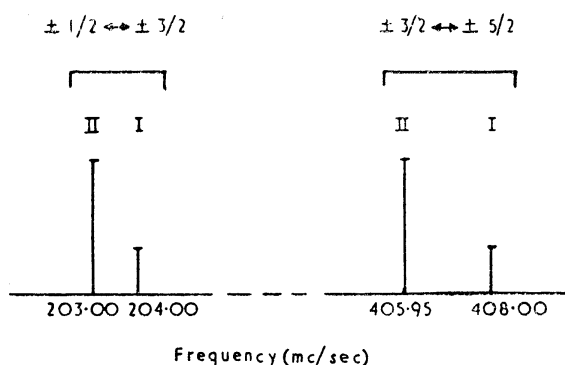


FIG. 6.—NQR spectrum of ^{127}I in SnI_4 .

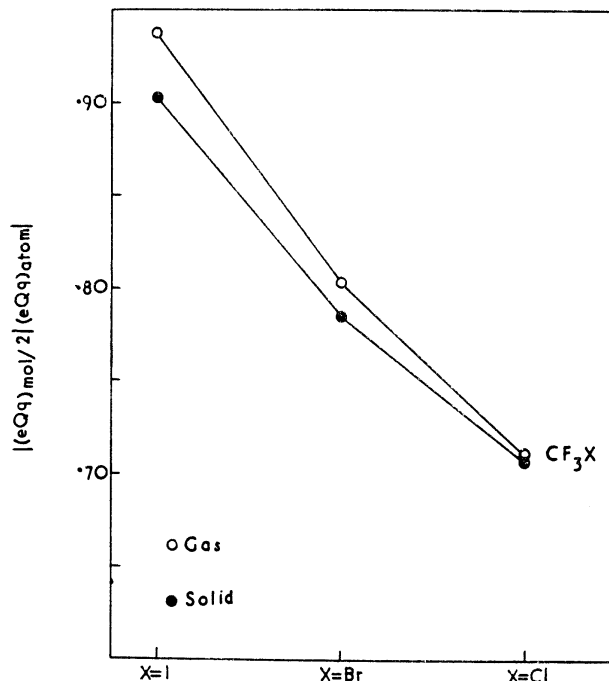
The doublet structure is explained by the occurrence of the two non-equivalent lattice sites I, II. The relative population and the local symmetry of these sites can be determined as 1:3 from the intensities and as trigonal or higher for I and lower than trigonal for II from the frequency ratios of the two ($I=5/2$) transitions $\pm 1/2 \leftrightarrow \pm 3/2$ and $\pm 3/2 \leftrightarrow \pm 5/2$.

covalent bonds with respect to the lattice,^{16, 22} as it depends strongly on the angle between the external magnetic field and the axes of the molecular electric field gradients. In quite a few cases these things can be learned comparatively easily from the NQR spectrum and then be used to simplify and corroborate the X-ray analysis of crystal structures.²³ A related application is the study of phase transitions^{24, 34} by observing the NQR spectrum while the temperature is changed.

We shall now proceed to cases where it is possible to make use of the coupling constants measured in the solid in a more refined way by comparing them with the corresponding couplings for the free atoms. One class of crystals interesting in this respect is that formed by the dipole-less element molecules and other highly symmetric molecules as far as they form molecular crystals held together only by weak van der Waals' forces. The very fact that these molecules have no dipole moments because of which they exhibit no rotational spectra insures here a minimum of interaction between neighbouring molecules. Nevertheless the concept of

non-interacting molecules in the solid state must of necessity only be an approximate one. Its justification, however, can be checked by sufficient other data, namely, low heat of sublimation, independence of associated Raman spectra on the state of aggregation and so on, not to mention the asymmetry parameter ϵ which for an end-atom forming a single bond should approach zero, and the narrowness of the multiple lattice site splitting of NQR lines mentioned earlier. There the theory of Townes and Dailey relating quadrupole coupling constants to molecular bonding can readily be applied. As discussed by Gordy in another paper presented at this meeting, one striking result to come out of work with crystals of this kind is the fact that the coupling constants for the molecular halogens, Cl_2 ,²⁵ Br_2 ,²⁶ I_2 ,^{16, 28} agree within a percent with the free atom values. This demonstrates that overlap effects must have but little influence on the density of the electron

FIG. 7.—Quadrupole coupling constant, molecular bonding and solid state perturbations. The decrease in the ratio of molecular to atomic coupling constant in the series CF_3I , CF_3Br , CF_3Cl , shows the increasing importance of ionic structures which do not contribute to the field gradient q . The correlation of decreasing intermolecular effects on the coupling in the solid with decreasing dipole moments is demonstrated also.



cloud around the nucleus, quite contrary to the predictions of present bonding theories. Appreciable experimental work has also been done on the tetrahalides.^{27, 28}

Besides in the nonpolar molecular crystals just discussed the situation of fairly weak interaction may also be expected for slightly polar constituents as, e.g., the organic halogen compounds. Comparison of the coupling constants for such molecules in the gaseous and the solid state usually show the differences to be not bigger than a few percent²⁸ and in selected cases it has even been possible to account for them in a satisfactory way.²⁹ Thus a large number of halogen compounds have been systematically investigated^{27, 28, 30} and it has been possible to correlate these data to molecular structure theories. Sometimes²⁰ it is possible to reduce the interaction between appreciable polar molecules (SbI_3) by the insertion of inert fillers (S_8) as²⁸ in $\text{SbI}_3 \cdot 3\text{S}_8$. This leads to studies of the effects of complex formation on quadrupole coupling which turned out to be rather small for SnCl_4 against $\text{SnCl}_4 \cdot \text{O}_2\text{NC}_6\text{H}_5$.³¹ The concept of well-defined isolated groups may even be extended to molecular ions like BrO_3^- and ClO_3^- in the corresponding metal salts. The NQR frequencies here have been shown to depend very little on the metal ion.²⁷

For crystals in which no clear-cut sub-groups can be identified and where the bonding between the atoms is intermediate between the covalent and ionic extremes

as, e.g., in SbCl_3 , the interpretation³² of the quadrupole coupling becomes exceedingly complex along with most other crystal properties. Cu_2O may represent a more favourable case³³ as it can be considered as a covalently bonded macromolecule. In this compound the Cu atom forms two clearly distinguishable linear covalent bonds after acquiring a positive charge of one.

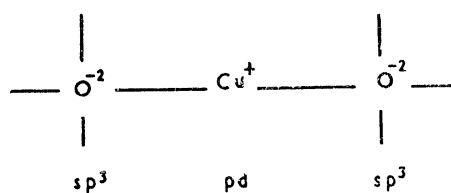


FIG. 8.—Bonding in the Cu_2O lattice.

The Cu^+ ion forms two linear bonds which can be explained as pd bonds derived from the excited $3d^94p$ configuration and give rise to a sizeable axial field gradient. In order to explain the 4 tetrahedral bonds formed by the O^{2-} ion as sp^3 bonds one has to assume the rather high excitation to the $2p^43s3p$ configuration.

In highly ionic crystals which contain atomic ions with filled electron shells NQR frequencies may sometimes be large enough for observation.³⁴ This is likely for heavier atoms with large couplings for low-lying excited states of the free ion, which may be sufficiently polarized by asymmetric surroundings. However, very few clues are available to estimate the expected NQR frequencies unless a NMR experiment with a suitable single crystal is performed. Therefore not much work has been done here.

TABLE 1

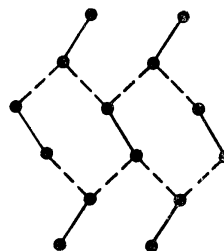
compound, quadrupole nucleus underlined	predominant electron configuration of quadrupole atom	NQR data			calculated from free atom data for pre- dominant configuration	
		ϵ %	eQq_{zz} Mc/s	ref.	eQq_{zz} Mc/s	ref.
$^{10}\text{B}(\text{CH}_3)_3$	$2s2p^2$	0	10.36	18	11.22	41
$^{10}\text{B}(\text{C}_2\text{H}_5)_3$	$2s2p^2$	0.9	10.43	18	11.22	41
IC^{14}N	$2s^22p^3$	0	3.40	19	0	
$^{14}\text{N}_4(\text{CH}_2)_6$	$2s^22p^3$	0	4.54	19	0	
$^{33}\text{S}_8$	$3s^23p^4$	—	45.8	35	—	
$^{35}\text{Cl}_2$	$3s^23p^5$	—	109.0	36	109.8	42
C^{35}Cl_4	$3s^23p^5$	—	81.9	30	109.8	42
$^{63}\text{Cu}_2\text{O}$	$3d^94p$	—	53.4	33	—	
$\text{K}[^{63}\text{Cu}(\text{CN})_2]$	$3d^{10}4s4p$	—	65.3	33	—	
$^{63}\text{Ga}_2\text{Cl}_6$	$4s4p^3$	—	58	37	0	
$^{75}\text{As}_4\text{O}_6$	$4s^24p^3$	—	232.5	38	0	
$^{79}\text{Br}_2$	$4s^24p^5$	—	765	26	769.8	43
$^{79}\text{BrCH}_3$	$4s^24p^5$	—	529	3	769.8	43
$\text{K}^{93}\text{NbO}_3$	$4s^24p^6$	80.6; 0	23.1; 16.0	34	0	
$^{123}\text{SbCl}_3$	$5s^25p^3$	19	489	32	0	
$^{127}\text{I}_2$	$5s^25p^5$	17.3	2153	16	2292	44
$\text{Sn}^{127}\text{I}_4$	$5s^25p^5$	0; 0.9	1363	16	2292	44
$^{201}\text{HgCl}_2$	$6s6p$	—	724	39	780	45, 46
$^{209}\text{Bi}(\text{C}_6\text{H}_5)_3$	$6s^26p^3$	8.9	669	40	0	

Knowledge of the experimental asymmetry parameter ϵ has been most helpful for the understanding of the bonding in solid iodine.^{28, 29} Experimental ϵ values also can be used to determine double bond character expected for theoretical reasons.²² A measurement of ϵ for the I atoms in BI_3 , e.g., should provide rather conclusive evidence for the 33 % double bond character demanded for the B—I bond by covalent bond theories.

A table of all atoms for which NQR has been observed so far giving the values of the coupling constant in one or two representative compounds as well as that calculated from free atom values for the predominant electron configurations used in the bond formation should round off this qualitative discussion of selected experimental work in NQR.

FIG. 9.—Bonding in solid I_2 .

The axial symmetry of the I_2 molecules—the intramolecular bond represented by a full line—is destroyed by the appreciable formation of weak intermolecular bonds—dashed lines ——. These additional bonds are responsible for the formation of infinite plane layers which, stacked over each other with rather wide spacing, make up the I_2 lattice.



The author is indebted to Dr. Walter Gordy for stimulating discussions. The help extended by the Bell Telephone Laboratories in preparing the manuscript is gratefully acknowledged.

- ¹ Dehmelt and Krüger, *Naturwiss.*, 1950, **37**, 111.
- ² Pound, *Physic. Rev.*, 1950, **79**, 655.
- ³ Dehmelt and Krüger, *Z. Physik*, 1951, **129**, 401.
- ⁴ Dehmelt, *Amer. J. Physics*, 1954, **22**, 110.
- ⁵ Bloembergen, Purcell and Pound, *Physic. Rev.*, 1948, **73**, 679.
- ⁶ Bloch, *Physic. Rev.*, 1946, **70**, 460.
- ⁷ Kellogg, Rabi, Ramsey and Zacharias, *Physic. Rev.*, 1939, **55**, 318.
- ⁸ Coles and Good, *Physic. Rev.*, 1946, **70**, 979.
- ⁹ Casimir, *On the Interaction between Atomic Nuclei and Electrons* (Bohn, Haarlem, 1936).
- ¹⁰ Casimir, *Physica*, 1935, **2**, 719.
- ¹¹ Krüger, *Z. Physik*, 1951, **130**, 371.
- ¹² Bersohn, *J. Chem. Physics*, 1952, **20**, 1505.
- ¹³ Cohen, *Physic. Rev.*, 1954, **96**, 1278.
- ¹⁴ Pound and Knight, *Rev. Sci. Instr.*, 1950, **21**, 219.
- ¹⁵ Livingston, *Ann. N. Y. Acad. Sci.*, 1952, **55**, 800.
- ¹⁶ Dehmelt, *Z. Physik*, 1951, **130**, 385.
- ¹⁷ Whitehead, *Superregenerative Receivers* (Cambridge University Press, Cambridge, 1950).
- ¹⁸ Dehmelt, *Z. Physik.*, 1952, **133**, 528 ; 1953, **134**, 642.
- ¹⁹ Watkins and Pound, *Physic. Rev.*, 1952, **85**, 1062.
- ²⁰ Townes and Dailey, *J. Chem. Physics*, 1949, **17**, 782.
- ²¹ Barnes and Smith, *Physic. Rev.*, 1954, **93**, 95.
- ²² Dean, *Physic. Rev.*, 1952, **86**, 607.
- ²³ Geller and Schawlow, to be published.
- ²⁴ Dean and Pound, *J. Chem. Physics*, 1952, **20**, 195.
- ²⁵ Livingston, *J. Chem. Physics*, 1951, **19**, 803.
- ²⁶ Dehmelt, *Z. Physik*, 1951, **130**, 480.
- ²⁷ Schawlow, *J. Chem. Physics*, 1954, **22**, 1211.
- ²⁸ Robinson, Dehmelt and Gordy, *J. Chem. Physics*, 1954, **22**, 511.
- ²⁹ Townes and Dailey, *J. Chem. Physics*, 1952, **20**, 35.
- ³⁰ Livingston, *J. Physic. Chem.*, 1953, **57**, 496.
- ³¹ Dehmelt, *J. Chem. Physics*, 1953, **21**, 380.
- ³² Dehmelt and Krüger, *Z. Physik*, 1951, **129**, 401.
- ³³ Krüger and Meyer-Berkhout, *Z. Physik*, 1952, **132**, 171.
- ³⁴ Cotts and Knight, *Physic. Rev.*, 1954, **96**, 1285.

- 35 Dehmelt *Physic. Rev.*, 1953, **91**, 313.
36 Livingston, *J. Chem. Physics*, 1951, **19**, 803.
37 Dehmelt, *Physic. Rev.*, 1953, **92**, 1240.
38 Krüger and Meyer-Berkhout, *Z. Physik*, 1952, **132**, 221.
39 Dehmelt, Robinson and Gordy, *Physic. Rev.*, 1954, **93**, 480.
40 Robinson, Dehmelt and Gordy, *Physic. Rev.*, 1953, **89**, 1305.
41 Wessel, *Physic. Rev.*, 1953, **92**, 1581.
42 Jaccarino and King, *Physic. Rev.*, 1951, **83**, 471.
43 King and Jaccarino, *Bull. Amer. Physic. Soc.*, 1953, **28**, 11.
44 Jaccarino, King, Satten and Stroke, *Physic. Rev.*, 1954, **94**, 1798.
45 Schuler and Schmidt, *Z. Physik*, 1935, **98**, 239.
46 Murakawa and Suwa, *J. Physic. Soc. Japan*, 1950, **5**, 429.